

Temperature dependence of the fundamental excitonic resonance in lead-salt quantum dots

Fangyu Yue, Jens W. Tamm, Detlef Kruschke, Bruno Ullrich, and Junhao Chu

Citation: [Applied Physics Letters](#) **107**, 022106 (2015); doi: 10.1063/1.4926806

View online: <http://dx.doi.org/10.1063/1.4926806>

View Table of Contents: <http://scitation.aip.org/content/aip/journal/apl/107/2?ver=pdfcov>

Published by the [AIP Publishing](#)

Articles you may be interested in

[Charge separation dynamics at bulk heterojunctions between poly\(3-hexylthiophene\) and PbS quantum dots](#)
J. Appl. Phys. **118**, 055502 (2015); 10.1063/1.4926869

[Size dependence of the polarizability and Haynes rule for an exciton bound to an ionized donor in a single spherical quantum dot](#)
J. Appl. Phys. **117**, 064309 (2015); 10.1063/1.4907760

[The role of surface defects in multi-exciton generation of lead selenide and silicon semiconductor quantum dots](#)
J. Chem. Phys. **136**, 064701 (2012); 10.1063/1.3682559

[Temperature dependence of electronic energy transfer in PbS quantum dot films](#)
Appl. Phys. Lett. **95**, 083102 (2009); 10.1063/1.3213349

[Temperature dependence of the photoluminescence emission from thiol-capped PbS quantum dots](#)
Appl. Phys. Lett. **90**, 101913 (2007); 10.1063/1.2711529

A promotional banner for Applied Physics Reviews. On the left is a small image of the journal cover for "Applied Physics Reviews" featuring a diagram of a device. The main part of the banner has a blue background with a bright light source on the right. The text "NEW Special Topic Sections" is prominently displayed in white. Below this, on an orange background, it says "NOW ONLINE" in yellow, followed by "Lithium Niobate Properties and Applications: Reviews of Emerging Trends" in white. The AIP Applied Physics Reviews logo is in the bottom right corner.

NEW Special Topic Sections

NOW ONLINE
Lithium Niobate Properties and Applications:
Reviews of Emerging Trends

AIP Applied Physics Reviews

Temperature dependence of the fundamental excitonic resonance in lead-salt quantum dots

Fangyu Yue,^{1,2} Jens W. Tomm,^{2,a)} Detlef Kruschke,³ Bruno Ullrich,⁴ and Junhao Chu^{1,5}

¹Key Laboratory of Polar Materials and Devices, Ministry of Education, East China Normal University, 500 Dongchuan Rd, Shanghai 200241, China

²Max-Born-Institut für Nichtlineare Optik und Kurzzeitspektroskopie, Max-Born-Str. 2A, 12489 Berlin, Germany

³Institut für Angewandte Photonik e.V. Rudower Chaussee 29/31, 12489 Berlin, Germany

⁴Instituto de Ciencias Físicas, Universidad Nacional Autónoma de México, Cuernavaca, Morelos 62210, Mexico and Ullrich Photonics LLC, Wayne, Ohio 43466, USA

⁵National Laboratory for Infrared Physics, Shanghai Institute of Technical Physics, 500 Yutian Rd, Shanghai 200083, China

(Received 27 March 2015; accepted 3 July 2015; published online 14 July 2015)

The temperature dependences of the fundamental excitonic resonance in PbS and PbSe quantum dots fabricated by various technologies are experimentally determined. Above ~ 150 K, sub-linearities of the temperature shifts and halfwidths are observed. This behavior is analyzed within the existing standard models. Concordant modeling, however, becomes possible only within the frame of a three-level system that takes into account both bright and dark excitonic states as well as phonon-assisted carrier redistribution between these states. Our results show that luminescence characterization of lead-salt quantum dots necessarily requires both low temperatures and excitation densities in order to provide reliable ensemble parameters. © 2015 AIP Publishing LLC.

[<http://dx.doi.org/10.1063/1.4926806>]

The accurate characterization of the optical properties of lead chalcogenide (e.g., PbS) quantum dots (QDs) is a prerequisite for their applications as narrow/broad bandwidth near infrared light source materials.^{1,2} Photoluminescence (PL) spectroscopy as a direct and effective tool is widely employed. For instance, based on the temperature dependence of the excitonic ground-state PL line (called E_x in the following) and full width at half maximum (W), key parameters including the temperature coefficient α ($=\partial E_x/\partial T$), the phonon energy (or temperature), and the (single) phonon coupling strength can be evaluated by referring to expressions, such as the Fan³ in Eq. (1) (or the Varshni in the limit of high temperature $k_B T \gg \hbar\omega$)⁴ for $E_x \sim T$ and Eq. (2) for $W \sim T$ (Refs. 3 and 4)

$$E_x(T) = E_0 + A(\langle N \rangle + \text{const}), \quad (1)$$

$$W(T) = \Gamma_0 + (\sigma T) + \Gamma_{LO} \langle N \rangle. \quad (2)$$

It is worth mentioning that these expressions are developed for bulk semiconductors representing almost ideal two-level systems and predict a near-to-linear evolution of E_x or W in the high temperature regime by following Bose-Einstein distribution with $\langle N \rangle = (e^{\hbar\omega/k_B T} - 1)^{-1}$. For confined lead salt QD systems, however, a three/multiple-level structure has been reported, e.g., due to electron-hole exchange interactions (or spin splitting).^{5,6} This different excitonic structure compared to bulk influences the distribution of carriers/excitons by additionally introduced relaxation channels and can result in a deviation from near-linear evolution of the parameters involved in Eqs. (1) and (2) at elevated temperatures, e.g., a sub-linear (or “saturation”)

behavior that has also been observed in absorption studies.⁷ This definitely influences the characterization of QDs and subsequently the derivation of related parameters, when the “standard” models are employed for parameter extraction. Up to now, no mechanism based on the excitonic fine structure of QDs is identified for this non-classic temperature-dependent evolution, but some phenomenological expressions are presented that allow to obtain decent fits to experimental data.^{7,8}

In this letter, we address the potential mechanisms of the temperature-dependent sub-linear behavior of the E_x -related emission parameters. A modified model being grounded on a Boltzmann-like distribution function is derived by referring to a three-level excitonic scheme and simultaneously considering the influence of the third level (e.g., a dark state) on the exciton-phonon coupling dynamics. Excellent fits to extensive experimental material deliver a universal behavior of the temperature dependence of the E_x -related parameters. The results also demonstrate that low temperatures and excitation densities are crucial in order to properly characterize lead salt QDs. This is important for any application.

Samples investigated here include colloidal⁹ and (boro-)silicate-glass-based¹⁰ PbX (X = S, Se) QDs (abbreviated as C_{PbX} or (B)G_{PbX}). PL was measured with a Bruker IFS-66v Fourier transform infrared (FTIR) spectrometer either by the rapid-scan or step-scan technique with pulsed or mechanically chopped 1064 nm radiation as excitation. As pointed out earlier,¹¹ the intensity of the optical excitation is critical and might induce extrinsic effects. Indeed, as confirmed here, very low excitation densities down to $\sim W/\text{cm}^2$ are required to observe undisturbed PL spectra. The measurements were performed from 5 K to 520 K.

^{a)}Electronic address: tomm@mbi-berlin.de

Figure 1(a) shows PL spectra of six typical samples at 5 K. From the figure, we can see that samples 1, 2, and 5 show fairly symmetric single PL peaks, while samples 3, 4, and 6 show multiple (or asymmetric) peaks. In case of samples 4 and 6, the asymmetry is caused by bimodal QD size distributions,⁹ which are designed to evaluate the influence of resonance energy transfer (FRET) between differently sized QDs. The triple-peak structure of sample 3 only appearing at low temperatures is related to the exciton ground-state split caused by the borosilicate glass matrix (with corresponding lifetimes of μ s, sub- μ s, and sub-100-ns order of magnitude from the low to high energy side; for details, see Ref. 12). For further analysis, attention will be paid to the main peaks (i.e., E_x -related peaks with a $\sim\mu$ s lifetime marked by arrows).

Figures 1(b) and 1(c) summarize the obtained values of E_x and W as a function of temperature. Obviously, all of them show a positive temperature dependence, i.e., an increase with temperature from 5 K to ambient. While in wide temperature ranges a linear behavior is observed, above 150 K also sub-linear behaviors are seen. This is independent of growth method, size distribution, and the presence of an exciton ground-state split. Exclusively, the part at low temperatures (e.g., below 150 K) can be described by standard models; see the dashes in Fig. 1(b) by Eq. (1) and Fig. 1(c) by Eq. (2). The values show a wide spread, and some of them show even significant inconsistency between Fan's and Varshni's approaches, e.g., (i) for PbS QDs, the temperature-coefficient $\alpha \in (68, 346)$ or $(73, 515)$ μ eV/K, of which the highest value by Varshni (with $E_0 \approx 0.8$ eV) almost exceeds that of bulk (~ 500 μ eV/K, Ref. 13); (ii) the average phonon energy $\bar{E}_p \in (2.5, 15.4)$ meV (with phonon temperature $\theta_p \in (29, 178)$ K), which almost covers the acoustic and LO phonon energy

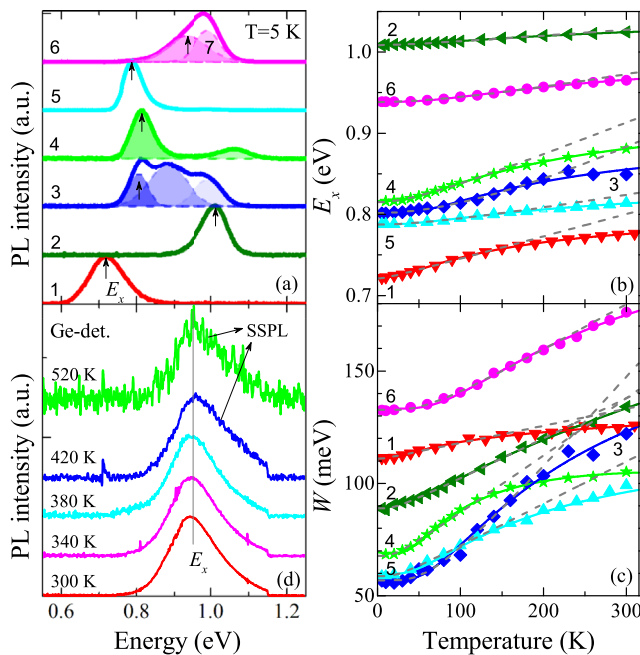


FIG. 1. (a) PL spectra and Gaussian-fit curves (dashes) of samples (1-G_{PbS}, 2-G_{PbS}, 3-BG_{PbS}, 4-C_{PbS}, 5-G_{PbSe}, and 6-G_{PbSe}) at 5 K. (b) and (c) Temperature dependence of the lowest excitonic E_x (b) and W (c) of samples. The dashed lines are predictions of standard models and the solid lines are fit results of the modified (Boltzmann-like) model. (d) Representative PL spectra of a sample at temperatures from 300 K to 520 K.

range; and (iii) the LO phonon energy $E_{LO} \in (1.5, 15.6)$ meV (with coupling coefficient $\Gamma_{LO} \in (1, 75)$ meV), part of which is smaller than the corresponding \bar{E}_p and even that of acoustic phonons; for more details, see Table I.

Direct evidence for a sub-linear behavior is given in Fig. 1(d), which shows the PL spectra measured at elevated temperatures up to 520 K. It is obvious that almost no change of E_x (and even W) can be observed within this extremely wide temperature range. Notice that the slight blue shift of E_x for Step-Scan FTIR PL (SSPL) in the figure, which is used to remove the background radiation of the ambient, is caused by the much higher excitation density compared to that when rapid-scan is used.

Now we come to the mechanisms and model that accounts for the observed sub-linear behavior. Note that the Fan parameter $A (= \alpha \theta_p)$ in Eq. (1) takes into account both the internal (electron-phonon interaction) and the external (thermal expansion) contributions to the dependence of $E_x(T)$.¹⁴ It can be then understood that the sub-linear behavior shown in Figs. 1(b) and 1(c) implies a net depletion of external thermal phonons (e.g., over 150 K) within the excitonic system.¹⁵ In this case, a model by referring to a non-classic two-level system can be presented to describe the sub-linear behavior, since the additionally introduced state(s) can involve the redistribution of the phonons. As shown in Fig. 2, it depicts the temperature dependent phonon coupling within the frame of a three-level system based on the presence of a split of the excitonic ground-state into a lower-lying dark/|D> state and a higher-lying bright/|B> state,¹⁶ where the |D> state provides a spontaneous relaxation channel for photo-excited excitons (even at extremely low temperatures with a temperature-independent rate of r_0). As the temperature increases (b), phonons can be activated, which on the one hand broaden E_x (for the case of positive α) by enhancing the |B>-related coupling (with a rate of r_1 of $|B\rangle \rightarrow |D\rangle$). On the other hand, they accelerate the activation process (r_2) of $|D\rangle \rightarrow |B\rangle$ (or “spin-flip” process) by depleting phonons,^{17,18} which may interrupt the classic behavior. The relaxation rate r_1 can be expressed as¹⁹

$$r_1 = r_0 + r_0 / (e^{\Delta/k_B T} - 1), \quad (3)$$

where Δ is the activation energy of $|D\rangle \rightarrow |B\rangle$, which for simplicity can be taken as $n\hbar\omega$ (n denotes the phonon number). The activation rate r_2 is as follows:

$$r_2 = r_0 / (e^{\Delta/k_B T} - 1) = r_1 e^{-\Delta/k_B T}. \quad (4)$$

It should be noted that the coefficient r_1 , which is frequently directly identified as r_0 (i.e., r_2 is r_1 -independent and only determined by Boltzmann-like statistics), represents that the temperature-dependent r_1 is mainly responsible for the number of |D>. At high temperatures, large r_1 increase r_2 , as reported elsewhere.²⁰ Therefore, in equilibrium, the contribution ratio f (or the competition factor between these two dynamic processes) of phonons to the |B>-related state can be expressed as a function of temperature²¹

$$f(T) = 1 - r_2/r_1 = 1 - e^{-\Delta/k_B T}, \quad (5)$$

by considering the advantages (i) to exclude the effect of intrinsic relaxation (i.e., r_0 , probably including the |D>-

TABLE I. Fit values obtained from Figs. 1(b) and 1(c) with Eqs. (10) and (12) (with $\sigma = 0$), respectively. Note that in the modified model $A \neq \alpha\theta_p$ and $\theta_p \approx 2\beta$. Sample 7 refers to the peak 7 in Fig. 1(a), which results in a negative α -value. Samples 8 and 9 are from the literature. For comparison, fitted values of samples 1–6 by Eq. (1) or Varshni and Eq. (2) are shown in brackets.

	E_0 (eV)	A (meV)	α ($\mu\text{eV/K}$)	θ_p (β) (K)	\bar{E}_p/Δ (meV)	Γ_0 (meV)	Γ_{LO} (meV)	E_{LO} (meV)
1 (G_{PbS})	0.722	76.8 (7.8)	393 (276)	119 (14)	10.3 (2.5)	111	19 (1)	8.7 (1.5)
2 (G_{PbS})	1.009	27.7 (4.7)	91 (73)	186 (51)	16.1 (5.9)	91	77 (10)	16.4 (4.9)
3 (BG_{PbS})	0.802	103.4 (58.9)	314 (515)	201 (289)	17.4 (15.4)	57	136 (75)	18.6 (15.6)
4 (C_{PbS})	0.816	107.4 (29.1)	398 (414)	162 (80)	14.0 (7.3)	69	54 (14)	8.5 (5.7)
5 (G_{PbSe})	0.789	47.0 (14.6)	142 (174)	190 (129)	16.4 (9.3)	60	65 (12)	14.3 (5.4)
6 (G_{PbSe})	0.939	58.9 (20.6)	123 (201)	239 (226)	20.6 (13.0)	133	103 (34)	23.4 (14.0)
7 (G_{PbSe})	0.995	52.0	−52	213	18.4	77	31	9.8
8 (G_{PbS}) ²²	0.887	106.0	339	186	16.1 (11.7 ^a)	69	101	28.2 \pm 2.2 (26.6 ^b)
9 (C_{PbSe}) ²³	0.821	97.0	295	204	17.6	42	113	13.4 \pm 0.3

^aFitted value in the literature.

^bThis value was fixed during fit process in the literature.

related relaxation rate), (ii) to neglect the different phonon coupling strengths for the $|B\rangle$ and $|D\rangle$ states, and (iii) to minimize the number of uncertain parameters.

It should be emphasized that this temperature-induced complex process resulting in $f(T)$ is due to the existence of the third level— $|D\rangle$ in the three-level system. This, however, substantially affects the redistribution of excitons/carriers (or phonons)²⁴ and therefore definitely changes the temperature-dependence of E_x -related parameters. This is not involved into a two-level system. It should be pointed out that the $f(T)$ in Eq. (5) can be alternatively deduced from multiple phonon-related non-radiative recombination rates between the two split levels, as reported by Andreakou *et al.*²⁵

$$r_1 = r_0[\langle N \rangle + 1]^{\Delta/\hbar\omega}, \quad (6)$$

$$r_2 = r_0\langle N \rangle^{\Delta/\hbar\omega}. \quad (7)$$

Here, $\Delta/\hbar\omega$ represents the phonon number. It hence demonstrates that the $f(T)$ derived from the activation/relaxation rates, which are basically derived from single-phonon coupling, also covers the case of multi-phonon coupling. As a result, Eq. (1) can be modified as done below by combining it with the effect of the dynamic process related to the third level

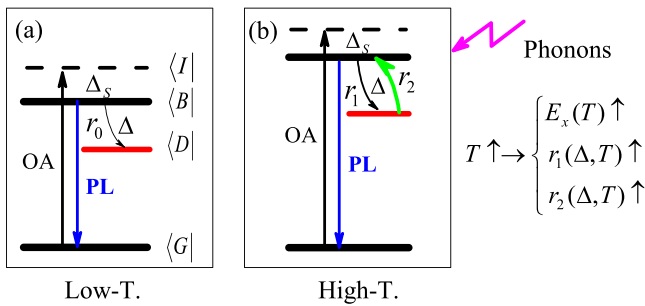


FIG. 2. (a) Three-level scheme with a bright/ $|B\rangle$, dark/ $|D\rangle$, and ground/ $|G\rangle$ exciton state. Δ is the activation energy of $|D\rangle$, which provides a spontaneous relaxation channel for $|B\rangle$ with a rate of r_0 . Δ_s is the Stokes shift between OA ($|I\rangle$) and PL. With temperature increase (b), exciton-phonon coupling gradually takes place. This increases E_x (with a positive α) and W and accelerates the relaxation of $|B\rangle$ with a rate of r_1 . It also activates $|D\rangle$ with a rate of r_2 . Note that in the two-level system the phonon coupling is mainly responsible for the variation of E_x .

$$\Delta E_x(T) = E_x(T) - E_0 = A(\langle N \rangle f(T) + \text{const}). \quad (8)$$

Note that the *const* has no effect on the temperature-dependent evolution, and the adjustable parameters E_0 ($T = 0$ K) and A can be treated as temperature-independent.¹⁴ So Eq. (8) can be re-expressed as

$$\Delta E_x(T) = A\langle N \rangle (1 - e^{-n\hbar\omega/k_B T}). \quad (9)$$

The “−” sign in the bracket can be understood from the ratio of phonons that come from the temperature increase but partially join the exciton-phonon coupling related to $|B\rangle$, which theoretically increases E_x (i.e., with a positive α). In other words, not all the temperature-induced phonons contribute to the broadening of the excitonic bandgap, if we take the excitonic fine structure as integral [see Fig. 2], since a portion is re-absorbed (i.e., annihilated) with a rate of r_2 to activate the $|D\rangle$ state with the increase of temperature (which will be also responsible for the following discussion about that elevated temperatures do not lead to the PL line broadening). Exactly, this in turn leads to the non-linear evolution of E_x -related parameters at elevated temperatures. A similar influence on the temperature dependence of bandgap was also observed elsewhere due to the activation of shallow levels.²⁶ Considering that the \bar{E}_p in lead salt QDs is comparable to the Δ -value, and the single-phonon coupling process is predominant due to the phonon bottleneck effect (i.e., $n = 1$),²⁷ Eq. (9) can be reduced to

$$\Delta E_x(T) = A e^{-\theta_p/T}. \quad (10)$$

Equation (10) follows Boltzmann-like statistics that is intrinsically different from the original Bose-Einstein pattern (see Eq. (1)). Notice that expressions like Eq. (10) have already been used for describing the $E_x \sim T$ relationship by other authors²⁸ without addressing the microscopic mechanisms involved.

Consequently, the influence of LO phonons contributing to the activation of $|D\rangle$ should also be taken into account. This is because their value of E_{LO} (~ 10 meV,²² 16 meV,²⁹ or 26 meV, Refs. 22 and 30) is fairly closer to the Δ -value than the ones of acoustic phonons (e.g., < 5 meV).¹⁷ Note that the fitted σ -value in Eq. (2) sometimes gives unphysical results,

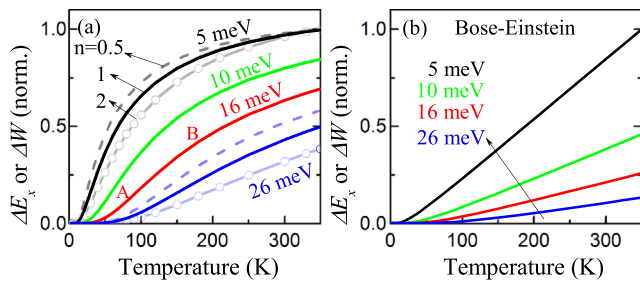


FIG. 3. Normalized temperature dependence of ΔE_x (with a positive α) or ΔW by following Boltzmann-like (a) and Bose-Einstein distributions (b). The predictions for typical phonon energies of 5 meV, 10 meV, 16 meV, and 26 meV are shown, and the n -value represents the possible phonon coupling number (e.g., $n = 1$ with solid lines).

in particular, a negative phonon coupling. Therefore, the second term can be omitted (i.e., $\sigma = 0$), since the contribution of acoustic phonons is involved due to the wide distribution of phonon frequency that is typical for lead salts.^{7,30} As a result, Eq. (2) can be modified as

$$\Delta W(T) = W(T) - \Gamma_0 = \Gamma_{LO} \langle N \rangle (1 - e^{-\hbar\omega/k_B T}). \quad (11)$$

And with $n = 1$, Eq. (11) can be simplified as

$$\Delta W(T) = \Gamma_{LO} e^{-E_{LO}/k_B T}. \quad (12)$$

It is important to mention that Eq. (12), similar to Eq. (10), has also been used to fit experimental data without giving reasonable microscopic motivation.^{20,31–34}

Figure 3 shows the results as obtained by the modified and standard models. Obviously, the modified model evolves towards sub-linearity at high temperatures (a), in contrast to the near-linear behavior of the standard model (b). In addition, Fig. 3(a) also indicates that (i) a smaller phonon energy (e.g., stronger acoustic phonon coupling) results in a more pronounced sub-linear behavior, i.e., a lower critical temperature point (cf. the point B) and (ii) a larger activation energy (Δ) causes a more linear relationship at high temperatures as standard models do, possibly because of the phonon-bottleneck.

To check the feasibility of our model, we fit the experimental data in Figs. 1(b) and 1(c) with Eqs. (10) and (12), respectively (see solid lines). It is evident that the modified model well describes the experimental evolutions in almost the entire temperature range. This is a substantial progress compared to the fit results obtained with the standard models (dashes). Table I gives the obtained parameters including the A , θ_p , and \bar{E}_p (or Δ), as well as the corresponding Γ_{LO} and E_{LO} . Note that the potentially additional broadening of W by the increased population of $|B\rangle$ with temperature is relatively small and can be omitted by considering the Δ value of ~ 10 – 20 meV. Note also that the A -value here has no standard Fan-relationship of $\alpha\theta_p$, and the α -value is deduced from the slope of the experimental data below θ_p (i.e., the slope of A–B range in Fig. 3(a) or referring to Varshni with $\beta = \theta_p/2$).³⁵

As shown in Table I, the excellent reproduction of the experimental data by the modified model yields also more realistic optical parameters compared to those from standard models. This involves (i) the α -value of QDs (91 – 398 $\mu\text{eV/K}$ for PbS and ~ 140 $\mu\text{eV/K}$ for PbSe) is significantly smaller

than that of bulk (~ 400 $\mu\text{eV/K}$ for PbSe³⁶) due to strong quantum confinement; (ii) the \bar{E}_p (or Δ) ranging within 10.3 – 20.6 meV, especially the $E_{LO} \in (8.5, 23.4)$ meV, is consistent with reports;^{7,37} (iii) the larger E_x (or smaller size) shows the larger splitting, and the Δ value for PbSe QDs with a stronger quantum confinement is larger compared to PbS QDs with a similar size; and (iv) more important, the \bar{E}_p obtained from $E_x \sim T$ is fairly comparable to the corresponding E_{LO} from $W \sim T$, except for those of bimodal QD samples (4, 6), which show a deviation. Note that the FRET between differently sized dots has been reported to significantly influence the evolution of QD optical parameters.^{2,9}

Moreover, our modified model allows for fitting of experimental data from literature (see samples 8 and 9 in Table I). However, part of the phonon energy yielded from $E_x \sim T$ does not match well that from $W \sim T$ because of the unclear excitation conditions (or potentially the size distribution), since the excitation intensity can intrinsically influence the temperature-dependence of PL peaks (including E_x , W , and Δ_s).^{11,38} This is also the reason why we emphasize the importance of low excitation density—in order to avoid any excitation-induced extrinsic mechanism. Notice that even for samples with a negative α -value, our model can well describe the experimental data; see sample 7 in Table I. For the inconsistency between the obtained \bar{E}_p (~ 18.4 meV) and E_{LO} (~ 9.8 meV), the FRET effect (between QDs in bimodal QD size distributions that have positive- and negative- α) can be regarded as a reason. We should point out that our modified model reasonably reproduces all experimental data, especially when the third ($|D\rangle$) state becomes effectively involved if $\Delta \approx \bar{E}_p$. In addition, it is important to mention that this model based on PL-related results can also describe the absorption spectral results; however, Dey *et al.*⁷ provides an alternative interpretation for the sub-linear behavior derived from absorption spectra by ascribing coupling to two different phonon modes with an opposite influence on the band-edge shift.

In summary, the temperature-dependent sub-linear behavior of the spectral position of the excitonic ground-state emission and its full width at half maximum for lead salt QDs has been addressed experimentally and theoretically. A modified model is proposed. It considers the activation dynamics of the third state in a three-level system. This model allows for describing the high-temperature behavior of the line position and halfwidth of the excitonic ground-state transition including deviations from a linear behavior at high temperatures. From a practical point of view, our results demonstrate that low temperatures and excitation densities are vital for proper PL characterization of this kind of QD systems.

The work was supported by the BMWi-Germany (MF090215), the NSFC (61376103 and 61474045) and the SHPP (15PJ1402200 and 78260024), and the DGAPA-UNAM-PAPIIT project TB100213-RR170213 (PI Bruno Ullrich).

¹F. Y. Yue, J. W. Tomm, D. Kruschke, and P. Glas, *Laser Photonics Rev.* **7**, L1 (2013).

²F. Y. Yue, J. W. Tomm, D. Kruschke, P. Glas, K. A. Bzheumikhov, and Z. C. Margushev, *Opt. Express* **21**, 2287 (2013).

³H. Fan, *Phys. Rev.* **82**, 900 (1951).

⁴I. Yeo, J. D. Song, and J. Lee, *Appl. Phys. Lett.* **99**, 151909 (2011).

- ⁵R. Espiau de Lamaestre, H. Bernas, D. Pacifici, G. Franzo, and F. Priolo, *Appl. Phys. Lett.* **88**, 181115 (2006).
- ⁶R. D. Schaller, S. A. Crooker, D. A. Bussian, J. M. Pietryga, J. Joo, and V. I. Klimov, *Phys. Rev. Lett.* **105**, 067403 (2010).
- ⁷P. Dey, J. Paul, J. Bylsma, D. Karaiskaj, J. M. Luther, M. C. Beard, and A. H. Romero, *Solid State Commun.* **165**, 49 (2013).
- ⁸H. J. Qiao, K. A. Abel, F. C. J. M. van Veggel, and J. F. Young, *Phys. Rev. B* **82**, 165435 (2010).
- ⁹J. S. Wang, B. Ullrich, G. J. Brown, and C. M. Wai, *Mater. Chem. Phys.* **141**, 195 (2013).
- ¹⁰I. Moreels, D. Kruschke, P. Glas, and J. W. Tomm, *Opt. Mater. Express* **2**, 496 (2012).
- ¹¹B. Ullrich and J. S. Wang, *Appl. Phys. Lett.* **102**, 071905 (2013).
- ¹²F. Y. Yue, J. W. Tomm, and D. Kruschke, *Phys. Rev. B* **89**, 081303(R) (2014).
- ¹³A. Olkhovets, R. C. Hsu, A. Lipovskii, and F. W. Wise, *Phys. Rev. Lett.* **81**, 3539 (1998).
- ¹⁴I. A. Vainshtein, A. F. Zatsypin, and V. S. Kortov, *Phys. Solid State* **41**, 905 (1999).
- ¹⁵S. Lüttjohann, C. Meier, M. Offer, A. Lorke, and H. Wiggers, *Europhys. Lett.* **79**, 37002 (2007).
- ¹⁶M. Nirmal, D. J. Norris, M. Kuno, and M. G. Bawendi, *Phys. Rev. Lett.* **75**, 3728 (1995).
- ¹⁷R. Matsunaga, Y. Miyauchi, K. Matsuda, and Y. Kanemitsu, *Phys. Rev. B* **80**, 115436 (2009).
- ¹⁸G. Schlegel, J. Bohnenberger, I. Potapova, and A. Mews, *Phys. Rev. Lett.* **88**, 137401 (2002).
- ¹⁹O. Labeau, P. Tamarat, and B. Lounis, *Phys. Rev. Lett.* **90**, 257404 (2003).
- ²⁰M. N. Nordin, J. Li, S. K. Clowes, and R. J. Curry, *Nanotechnology* **23**, 275701 (2012).
- ²¹As another way to understand the influence of $|D\rangle$, in equilibrium the competition between $|B\rangle$ and $|D\rangle$ (or the ratio of $|D\rangle$ being activated) can be presented as a function of temperature, $r(T) = r_2/r_1 = \exp(-\Delta/k_B T)$, by considering (i) to involve the influence of dynamic recombination rates (strictly the phonon distribution with temperature) on the *const* in Eq. (1) and (ii) to avoid the effect of r_0 and minimize the number of uncertain parameters. Note that the $r(T)$ based on Eqs. (3) and (4) (single-phonon coupling) can also be deduced from Eqs. (6) and (7) (multiple-phonon coupling). Then, the *const* in Eq. (1) can be modified by combining with the influence of the dynamic process related to $|D\rangle$, $const = r(T)\langle N \rangle = \langle N \rangle \exp(-\Delta/k_B T)$. Subsequently, Eqs. (9)–(12) can be deduced if we understand the *const* as the **consumption** of phonons for activating $|D\rangle$ (as described in the text). Note also that in standard models the rate relationship between $|B\rangle$ and $|D\rangle$ taken as $r(T) = |r_2 - r_1| = r_0$ (from Eqs. (3) and (4)) is temperature-independent, obviously inconsistent with the essence of three-level QDs ($|r_2 - r_1| \neq r_0$ from Eqs. (6) and (7) also implies the unreasonableness of the standard assumption).
- ²²M. S. Gaponenko, A. A. Lutich, N. A. Tolstik, A. A. Onushchenko, A. M. Malyarevich, E. P. Petrov, and K. V. Yumashev, *Phys. Rev. B* **82**, 125320 (2010).
- ²³A. Kigel, M. Brumer, G. I. Maikov, A. Sashchiuk, and E. Lifshitz, *Small* **5**, 1675 (2009).
- ²⁴H. E. Chappell, B. K. Hughes, M. C. Beard, A. J. Nozik, and J. C. Johnson, *J. Phys. Chem. Lett.* **2**, 889 (2011).
- ²⁵P. Andreakou, M. Brossard, C. Li, M. Bernechea, G. Konstantatos, and P. G. Lagoudakis, *J. Phys. Chem. C* **117**, 1887 (2013).
- ²⁶F. Y. Yue, J. Shao, X. Lü, W. Huang, J. H. Chu, J. Wu, X. C. Lin, and L. He, *Appl. Phys. Lett.* **89**, 021912 (2006).
- ²⁷V. I. Klimov and D. W. McBranch, *Phys. Rev. Lett.* **80**, 4028 (1998).
- ²⁸M. A. da Silva, I. F. Dias, J. L. Duarte, E. Laureto, I. Silvestre, L. A. Cury, and P. S. Guimaraes, *J. Chem. Phys.* **128**, 094902 (2008).
- ²⁹B. Ullrich, X. Y. Xiao, and G. J. Brown, *J. Appl. Phys.* **108**, 013525 (2010).
- ³⁰T. D. Krauss and F. W. Wise, *Phys. Rev. Lett.* **79**, 5102 (1997).
- ³¹A. Al Salman, A. Tortschanoff, M. B. Mohamed, D. Tonti, F. van Mourik, and M. Chergui, *Appl. Phys. Lett.* **90**, 093104 (2007).
- ³²J. Lee, E. Koteles, and M. Vassell, *Phys. Rev. B* **33**, 5512 (1986).
- ³³C. Kammerer, C. Voisin, G. Cassaboïs, C. Delalande, P. Roussignol, F. Kloppe, J. P. Reithmaier, A. Forchel, and J. M. Gerard, *Phys. Rev. B* **66**, 041306(R) (2002).
- ³⁴S. Rudin, T. Reinecke, and B. Segall, *Phys. Rev. B* **42**, 11218 (1990).
- ³⁵O. Kopylov, J. Lee, I. Han, W. J. Choi, J. D. Song, and I. Yeo, *J. Korean Phys. Soc.* **60**, 1828 (2012).
- ³⁶I. A. Smirnov, B. Y. Moizhes, and E. D. Nensberg, *Sov. Phys. Solid State* **2**, 1793 (1961).
- ³⁷B. Ullrich, J. S. Wang, and G. J. Brown, *Appl. Phys. Lett.* **99**, 081901 (2011).
- ³⁸B. Ullrich, H. Xi, and J. S. Wang, *J. Appl. Phys.* **115**, 233503 (2014).